JOURNAL OF OPTOELECTRONICS AND ADVANCED MATERIALS Vol. 12, No. 3, March 2010, p. 535 - 537

Investigations of microstructural evolutions after rapid thermal annealing of phosphorus doped ZnO films grown by pulsed laser deposition

J. H. JANG[a], H. S. KIM[b], D. P. NORTON[a], V. CRACIUN[a,c,*]
[a]*Department of Materials Science and Engineering, University of Florida, Box 116400, Gainesville, FL 32611*
[b]*Oak Ridge National Laboratory, Box 2008 MS6056, Oak Ridge, TN 37831*
[c]*Laser Department, National Institute for Laser, Plasma, and Radiation Physics, Bucharest, Romania*

The microstructure of as-deposited and rapid thermal annealed (RTA) P-doped ZnO films grown by pulsed laser deposition (PLD) on c-plane sapphire substrates was investigated. Omega rocking curve (ω-RC) and pole figure investigations showed that the degree of texture and crystalline quality of films decreased with increasing phosphorus concentration. X-ray diffraction line profile analysis (LPA) and Warren–Averbach analysis showed that 0.5 at % P-doped ZnO film presented much higher microstrain values than 1.0 at % P-doped ZnO films, which indicated that phosphorus atoms are no longer incorporated into the ZnO lattice for such concentrations. After RTA at 900 °C for 3 min, the FWHM values of ω-RCs markedly decreased, indicating a significant improvement of crystallinity. In addition, the change of the conduction type from n to p simultaneously with a decrease of strain suggested that P atoms were incorporated back into the ZnO lattice.

(Received June 19, 2009; accepted October 23, 2009)

Keywords: Laser ablation, ZnO, Microstructure

1. Introduction

ZnO is one of the most promising material for optoelectronics device applications due to its wide bandgap energy (3.37 eV) and large exciton binding energy (60 meV) [1-3]. However, despite many studies it is very difficult to produce p-type ZnO films because of the deep level location of the candidate acceptors from ZnO valence band and their self-compensation by native point defects [4,5]. Phosphorus (P) attracted an extensive attention as a p-type dopant in ZnO [6-8] and it was reported that rectifying and light emitting diodes were realized with phosphorus doped ZnO films [9,10]. The growth conditions, such as growth temperature, O_2 partial pressure, substrate treatment and so on, have a strong influence on the crystalline quality of the ZnO films, as many studies pointed out [11-13]. However, a detailed study on the microstructure of the P-doped ZnO films has only recently been performed [14]. The results showed that for P doping concentration as low as 1 at % there is a strong segregation effect that degrades the crystalline structure. In this letter, we report a comparison between the structure of as-grown and rapid thermal annealed undoped and 0.5, and 1.0 at % P-doped ZnO films grown on the c-plane sapphire substrate.

2. Experiments

Details about the deposition and characterization of ZnO:P films were recently published [14] and are only briefly mentioned here. The layers were grown on c-plane sapphire substrates by the pulsed laser deposition (PLD) technique at 700 °C in an oxygen partial pressure of 150 mTorr. Prior to ZnO:P deposition, an undoped ZnO buffer layer was firstly deposited at 400 °C in 20 mTorr of O_2 and then annealed at 650 °C in an oxygen ambient. Two phosphorous-doped ZnO targets containing 0.5 and 1 at. % P were fabricated using high-purity ZnO (99.9995 %) mixed with P_2O_5 (99.998 %). The targets were ablated by a KrF excimer laser working with a pulse repetition rate of 1 Hz and an energy density of approximately 1.5 J/cm^2. The film thickness was approximately 400 nm for the ZnO:P layer and 100 nm for the undoped ZnO buffer layer. After deposition, films underwent a Rapid Thermal Annealing (RTA) process under high purity oxygen at 900 °C for 3 min.

The microstructure of grown films was examined by a Panalytical MRD X'Pert system equipped with a 1/2° slit, mirror and Ge (220) monochromator on the primary optics and a channel cut Ge (220) analyzer on the secondary optics (parallel beam geometry) and in a Philips APD3720 using the Bragg-Brentano (focusing) geometry. The room temperature electrical properties were investigated by Hall effect measurements using the four-point van der Pauw geometry with a commercial LakeShore Hall measurement system [15].

3. Results and discussion

By analyzing the $\{10\bar{1}1\}$ pole figures recorded from as-grown undoped, 0.5, and 1.0 at. % P-doped ZnO films it was inferred [14] that the ZnO films are textured along the c-axis, the preferred way of ZnO films growth by PLD [15-18]. It was also apparent that the degree of texture degraded with increasing phosphorus atomic percent in ZnO.

Interestingly, it was also found from the pole figure that there are two columnar structures, which were identified from the $\{10\bar{1}1\}$ and $\{10\bar{1}4\}$ phi (ϕ)-scans of ZnO films and sapphire substrate, respectively, as $ZnO[10\bar{1}0]//Al_2O_3[11\bar{2}0]$ and $ZnO[10\bar{1}0]//Al_2O_3[10\bar{1}0]$. The $ZnO[10\bar{1}0]//Al_2O_3[11\bar{2}0]$ orientation corresponded to a film that exhibited narrower ϕ-scan peak widths than those measured for films aligned with the substrate because the 30° in-plane rotation with respect to the sapphire substrate decreases the lattice mismatch (18.4%).

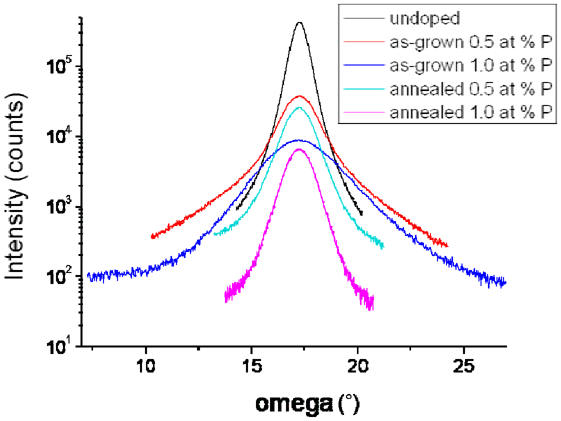

Fig. 1. (0002) ω-RCs measured from the grown and annealed samples.

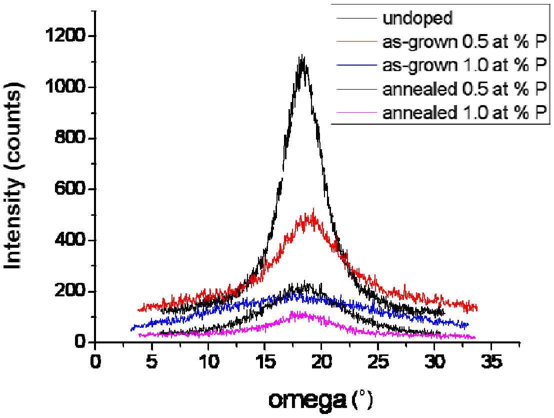

Fig. 2. $(10\bar{1}1)$ *ω-RCs measured from the grown and annealed samples.*

Figs. 1 and 2 display the omega rocking curves (ω-RCs) recorded to investigate the crystalline quality of the grown films. Both the (0002) and $(10\bar{1}1)$ ω-RCs were measured in symmetric and skew geometry, respectively. For all samples the (0002) ω-RC showed higher intensity and smaller full width at half maximum (FWHM) values than the $(10\bar{1}1)$ ω-RCs.

Table 1. ω-RCs FWHM values measured from the deposited and RTA processed films.

Sample	ω-RCs FWHM (°)	
	(0002)	$(10\bar{1}1)$
undoped	0.779	4.209
as-grown 0.5 at. % P	1.683	7.082
as-grown 1.0 at. % P	3.235	19.148
annealed 0.5 at. % P	1.410	8.223
annealed 1.0 at. % P	1.327	6.486

This is an indication that the in-plane columnar domains are twisted with a certain angle due to the presence of threading dislocations, resulting in the formation of the low angle grain boundary. It is worth noting that the ω-RC FWHM values improved dramatically after the RTA process, the 1 at % P sample exhibiting narrower values than the 0.5 at % P , as shown in Table 1.

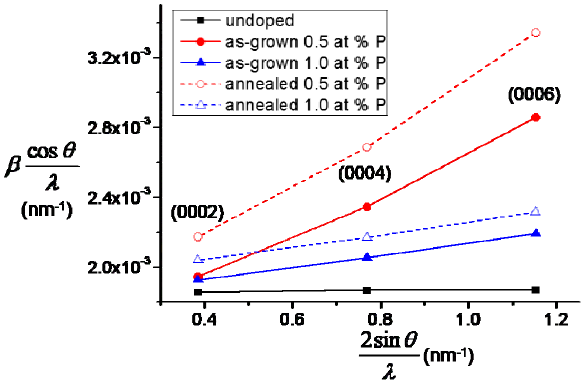

Fig. 3. Williamson–Hall plot for deposited films.

For further analysis of the microstructure of P-doped ZnO films, an x-ray diffraction line profile analysis (LPA) study was performed. Several {0001} diffraction lines were recorded in a $\theta/2\theta$ scan mode and their FWHM were measured. By plotting $\beta.\frac{\cos\theta}{\lambda}$ versus $\frac{2\sin\theta}{\lambda}$, in which β is integral breadth, θ is Bragg angle, and λ is X-ray wavelength, a Williamson-Hall plot [19] is obtained, which is shown in Fig. 3. The values of average crystallite size ($<D>_V$) and the r.m.s. strain (ε_{rms}) estimated from the Williamson-Hall plot are displayed in Table II. The same parameters were estimated using the Warren-Averbach method for the (0002) and (0004) lines and presented in Table III for completeness sake. One can note that while the crystallite size is rather similar at around 500~600 Å for all ZnO samples, the 0.5 at % P-doped ZnO film shows the highest microstrain, both for the as-grown as for the annealed samples.

Table 2. Results obtained from Williamson – Hall plot for grown films.

	undoped	as-grown P-doped ZnO		annealed P-doped ZnO	
P atomic %	0	0.5	1.0	0.5	1.0
Strain (%)	0.002	0.119	0.035	0.152	0.036
Crystallite size (Å)	540	680	558	641	526

Table 3. Results obtained from Warren-Averbach analysis of deposited films.

	undoped	as-grown P-doped ZnO		annealed P-doped ZnO	
P atomic %	0	0.5	1.0	0.5	1.0
Strain (%)	0.038	0.072	0.059	0.11	0.08
Crystallite size (Å)	550	618	535	415	472

It is believed that P atoms incorporation into the ZnO lattice must generate an internal strain. Therefore, one can argue, based on the X-ray diffraction line profile analysis, that the P atoms were effectively incorporated into the ZnO lattice for the sample with 0.5 at % P, resulting in the highest strain. From the Hall measurement, the 1.0 at % P-doped ZnO film showed a lower carrier density than the 0.5 at % P-doped ZnO film ($1.8\times10^{17}cm^{-3}$ versus $6.2\times10^{17}cm^{-3}$) which is also consistent with a lower substitutional incorporation, confirming the results of the X-ray diffraction line profile analysis and our previous x-ray photoelectron spectroscopy (XPS) investigations [14]. However, the behavior of annealed samples is somehow puzzling, deserving further analysis. The FWHM values of ω-RCs significantly decreased indicative of a much better crystallinity. However, the strain values slightly increased, more so for the 0.5 at % P sample. The fact that the type of the conductivity changes after the RTA process from n to p-type [15] for these samples is consistent with substitutional incorporation of P atoms into the ZnO lattice.

4. Conclusions

The microstructure of as-deposited and rapid thermal annealed P-doped ZnO films with different phosphorus atomic percent was investigated. The results indicated that a significant fraction of phosphorus atoms in 1.0 at % P-doped ZnO film are segregated while in 0.5 at % P-doped ZnO film they are effectively incorporated into ZnO lattice, resulting in a high internal strain. However, to achieve p-type conduction an additional RTA process at 900 °C was required.

Acknowledgements

The authors would like to thank Major Analytical Instrumental Center (MAIC), University of Florida for help with characterization. This work was partially funded by CNCSIS Ideas project 421.

References

[1] Z. K. Tang, G. K. L. Wong, P. Yu, Appl. Phys. Lett., **72**, 3270 (1998).
[2] H. Ohota, K. Kawamura, M. Orita, M. Hirano, N. Sarukura, H. Hosono, Appl. Phys. Lett., **77**, 475 (2000).
[3] D. M. Bagnall, Y. F. Chen, Z. Zhu, T. Yao, S. Koyama, M. Y. Shen, T. Goto, Appl. Phys. Lett., **70**, 2230 (1997).
[4] D. C. Look, D. C. Reynolds, C. W. Litton, R. L. Jones, D. B. Eason, G. Cantwell, Appl. Phys. Lett., **81**, 1830 (2002).
[5] C. G. Van de Walle, Phys. Rev. Lett., **85**, 1012 (2000).
[6] C. H. Park, S. B. Zhang, S. H. Wei, Phys. Rev. B **66**, 073202 (2002).
[7] M. Pan, J. Nause, V. Rengarajan, R. Rondon, E. H. Park, I. T. Ferguson, J. Electron. Mater. **36**, 457 (2007).
[8] S. Yamauchi, Y. Goto, T. Hariu, J. Cryst. Growth, **260**, 1 (2004).
[9] K. Ip, Y. W. Heo, D. P. Norton, S. J. Pearton, J. R. LaRoche, F. Ren, Appl. Phys. Lett., **85**, 1169 (2004).
[10] J. –H. Lim, C. –K. Kang, K. –K. Kim, I. –K. Park, D. –K. Hwang, S. –J. Park, Adv. Mater. **18**, 2720 (2006).
[11] C. Liu, S. H. Chang, T. W. Noh, M. Abouzaid, P. Ruterana, H. H. Lee, D. –W Kim, J. –S. Chung, Appl. Phys. Lett. **90**, 011906 (2007).
[12] T. –B. Hur, Y. –H. Hwang, H. –K. Kim, H. –L Park, J. Appl. Phys., **96**, 1740 (2004).
[13] Y. Chen, D. M. Bagnall, H. Koh, K. Park, K. Hiraga, Z. Zhu, T. Yao, J. Appl. Phys., **84**, 3912 (1998).
[14] J.H. Jang, H.S. Kim, D.P. Norton V. Craciun, Journal of Crystal Growth, **311**, 3143 (2009).
[15] H. S. Kim, S. J. Pearton, D. P. Norton, J. Appl. Phys., **102**, 104904 (2007).
[16] R. D. Vispute, V. Talyansky, S. Choopun, R. P. Sharma, T. Venkatesan, M. He, X. Tang, J. B. Halpern, M. G. Spencer, Y. X. Li, L. G. Salamanca-Riba, A. A. Iliadis, K. A. Jones, Appl. Phys. Lett., **73**, 348 (1998).
[17] V. Craciun, J. Perriere, N. Bassim, R. K. Singh, D. Craciun, J. Spear, Appl. Phys. A **69**, S531 (1999)
[18] V. Craciun, R. K. Singh, J. Perriere, J. Spear, D. Craciun, J. Electrochemical Society, **147**, 1077 (2000)
[19] G.. K. Williamson, W. H. Hall, Acta. Metall., **1**, 22 (1953).

---

[*] Corresponding author: vcrac@mse.ufl.edu